Method of Moments Analysis of Anisotropic Artificial Media Composed of Dielectric Wire Objects

Matthew E. Peters, *Member, IEEE*, and Edward H. Newman, *Fellow, IEEE*

***Abstract*—The paper considers the periodic method of moments (PMM) analysis of anisotropic artificial media composed of a 3-D periodic array of identical scatterers. The method is based upon finding the complex wavenumber(s), and the eigenfunction currents and fields, for a plane wave propagating in the artificial medium. From these quantities, the effective tensor constitutive parameters are determined. It is shown that for a given direction of propagation through an artificial medium, there are two distinct modes of plane wave propagation, which may change with the direction of propagation. Examples are shown for the case where the periodic scatterers are thin dielectric wire structures.**

I. Introduction

An artificial medium is basically a macroscopic analog of a real medium [1, ch. 12], and typically consists of a large number of scattering objects distributed (more or less) uniformly in some host or background medium. For simplicity of analysis, here the artificial medium is assumed to be composed of a 3-D infinite periodic array of identical scattering elements. When a plane wave propagates through an artificial medium, currents are induced in (or on) the scattering objects. These currents can be viewed as macroscopic current moments, analogous to the microscopic dipole moments induced in the molecules of a real dielectric [2]. The effect of the macroscopic current moments is to produce a net electric and magnetic current moment per unit volume, giving the artificial medium some complex effective tensor permittivity and permeability different from that of the host medium. The complex effective constitutive parameters of the artificial medium are a function of frequency, the electrical size, shape, spacing, and orientation of the scattering objects, and the constitutive parameters of both the host medium and the scattering objects. By properly choosing the geometry and composition, it may be possible to design an artificial medium of desired permittivity, permeability and loss tangent. This paper reviews the periodic method of moments (PMM) analysis of artificial media, and presents examples for 3-D periodic structures of material wire scatterers. The reader is referred to the authors previous work [3], [4] and to Collin's book [1] for a bibliography on artificial media.

The PMM analysis of artificial media proceeds as follows. First, a homogeneous integral equation is formulated for a plane wave of unknown wavenumber propagating in a periodic artificial medium of infinite extent in all three dimensions. Next, this integral equation is solved by the PMM, yielding the complex effective wavenumbers of the plane wave, the eigenfunction currents in the wire objects, and the eigenfunction fields in the artificial medium. From these quantities, the effective constitutive parameters of the artificial medium are determined. The principle advantage of the PMM solution is that it is a full wave solution and accounts for how mutual coupling can effect the *shape* of the currents on the scatterers in the periodic array. This change in the shape of the current can be extremely important, especially for very closely spaced elements [3], [4, Figs. 11 and 12].

Manuscript received May 20, 1994; revised May 25, 1995. This work was sponsored by The Joint Services Electronics Program Contract N00014-78-C-0049 with the Ohio State University Research Foundation.

The authors are with The Ohio State University, ElectroScience Laboratory, Columbus, OH 43212 USA.

IEEE Log Number 9413419.

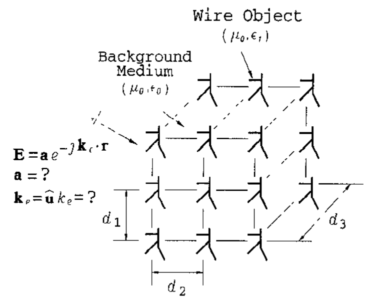

Fig. 1. Geometry of the general artificial dielectric.

II. Theory

As shown in Fig. 1, the geometry of the artificial medium consists of a 3-D triple infinite periodic array of dielectric wire objects located in a homogeneous and isotropic host medium. The homogeneous host medium has constitutive parameters (μ_0, ϵ_0), wavelength λ_0, wavenumber k_0, and is not necessarily free space and may be lossy. The thin wire objects [6] may be composed of an arbitrary conductive or dielectric material, and are arranged in a rectangular lattice cell structure with spacings d_1, d_2, and d_3 in the $\hat{\boldsymbol{x}}, \hat{\boldsymbol{y}}$, and $\hat{\boldsymbol{z}}$ directions, respectively. The reference or center cell is centered at the origin. All fields and currents are time harmonic with the $e^{j\omega t}$ time dependence suppressed.

As has been previously published by the authors [3]–[5], the periodic moment method (PMM) is used to determine the wavenumber(s) for a plane wave propagating in a given direction (without excitation) in the artificial medium. The plane wave fields have spatial variation of the form

$$e^{-j\boldsymbol{k}_e \cdot \boldsymbol{r}} \tag{1}$$

where $\boldsymbol{k}_e = k_e\hat{\boldsymbol{u}}$ is the unknown vector wavenumber of the plane wave propagating in the known $\hat{\boldsymbol{u}}$ direction, and $\boldsymbol{r}$ is the position vector. Assuming that the current on the scatterers is expanded in terms of N basis functions, the PMM solution results in a homogeneous matrix equation of the form

$$[\mathcal{Z}(k_e)]I = 0 \tag{2}$$

where $[\mathcal{Z}(k_e)]$ is the order N impedance matrix, and I is the length N current vector which contains the N unknown coefficients in the expansion for the current on the center or reference element. Equation (2) has a non–trivial solution only if the determinant of the impedance matrix is zero. Thus, k_e is found by an iterative solution of the fundamental equation

$$|\mathcal{Z}(k_e)| = 0. \tag{3}$$

Generally, there are two distinct roots to (3); however, in certain special cases one root is a free space root ($k_e = k_0$), while in other cases the two roots are identical due to array symmetry. Associated with each root there is a polarization $\hat{\boldsymbol{u}}$ and eigenfunction currents and fields. From these values, the effective permeability and permittivity $(\overline{\mu}_e, \overline{\epsilon}_e)$ can be determined.

A. Evaluation of the Effective Constitutive Parameters

This section presents a new method, termed Maxwell's Equations method [4], for determining the dyadic effective permittivity and permeability $(\overline{\epsilon}_e, \overline{\mu}_e)$ of an anisotropic artificial medium. Also, two methods previously published by the authors [3]–[5] are briefly summarized. It is assumed that for a given geometry, the two roots k_e of (3), their corresponding eigenfunction currents $\boldsymbol{J}^0$ on the center element, and their eigenfunction fields averaged over the volume of the center cell $(\boldsymbol{E}^0, \boldsymbol{H}^0)$, have all been determined.

1) Maxwell's Equations Method: Maxwell's Equations method determines the effective tensor constitutive parameters of the artificial medium such that the eigenfunction fields averaged over the center cell, $(\boldsymbol{E}^0, \boldsymbol{H}^0)$. satisfy Maxwell's source free equations [4]. For a plane wave of the form of (1), Maxwell's differential equations reduce to the algebraic equations [7, section 2.3]

$$\begin{aligned} \nabla \times \boldsymbol{H} = -j\omega \boldsymbol{D} \Rightarrow \boldsymbol{k}_e \times \boldsymbol{H}^0 &= -\omega \boldsymbol{D}^0 \\ &= -\omega \overline{\epsilon}_e \cdot \boldsymbol{E}^0 \end{aligned} \tag{4}$$

$$\begin{aligned} \nabla \times \boldsymbol{E} = j\omega \boldsymbol{B} \Rightarrow \boldsymbol{k}_e \times \boldsymbol{E}^0 &= \omega \boldsymbol{B}^0 \\ &= \omega \overline{\mu}_e \cdot \boldsymbol{H}^0. \end{aligned} \tag{5}$$

Equation (4) can be explicitly shown as the order 3 matrix equation

$$\begin{bmatrix} k_{ey}H_z^0 - k_{ez}H_y^0 \\ k_{ez}H_x^0 - k_{ex}H_z^0 \\ k_{ex}H_y^0 - k_{ey}H_x^0 \end{bmatrix} = -\omega \begin{bmatrix} \epsilon_{xx}^e & \epsilon_{xy}^e & \epsilon_{xz}^e \\ \epsilon_{yx}^e & \epsilon_{yy}^e & \epsilon_{yz}^e \\ \epsilon_{zx}^e & \epsilon_{zy}^e & \epsilon_{zz}^e \end{bmatrix} \begin{bmatrix} E_x^0 \\ E_y^0 \\ E_z^0 \end{bmatrix} \tag{6}$$

relating the nine components of the permittivity dyad to the average electric and magnetic fields in the center cell. Equation (6) is equivalent to three equations in the nine components of $\overline{\epsilon}_e$, and is the result of one of the two roots of (3). The other root will produce a dyadic equation, similar to (6) *with the same* $\overline{\epsilon}_e$, but with different $\boldsymbol{k}_e$ and $(\boldsymbol{E}^0, \boldsymbol{H}^0)$. The two dyadic equations, along with the condition that $\overline{\epsilon}_e$ is symmetric, can now be used to solve for the nine components of $\overline{\epsilon}_e$. The determination of $\overline{\mu}_e$ is parallel to that presented for $\overline{\epsilon}_e$, but uses the dyadic (5).

2) Polarization Method: The polarization method [3], [4] enforces the constitutive relationships in an average sense over the center cell. Denoting $\boldsymbol{P}^0$ and $\boldsymbol{M}^0$ as the electric and magnetic dipole moment per unit volume averaged over the center cell, the constitutive relationships become

$$\boldsymbol{D}^0 = \epsilon_0 \boldsymbol{E}^0 + \boldsymbol{P}^0 = \overline{\epsilon}_e \cdot \boldsymbol{E}^0 \tag{7}$$

$$\boldsymbol{B}^0 = \mu_0(\boldsymbol{H}^0 + \boldsymbol{M}^0) = \overline{\mu}_e \cdot \boldsymbol{H}^0 \tag{8}$$

and are used in place of (4) and (5).

3) Simple Uniaxial Formula: Uniaxial media are characterized by diagonal $\overline{\mu}_e$ and $\overline{\epsilon}_e$. When propagation is along a given principle axis, the two roots of (3) correspond to the polarization in the directions of the two principle axes transverse to the direction of propagation. For a given root k_e one can compute the average fields $(\boldsymbol{E}^0, \boldsymbol{H}^0)$ and then the corresponding wave impedance η_e as the ratio of the tangential electric to magnetic fields. The parameters μ_e and ϵ_e are related to k_e and η_e through the relations

$$k_e = \omega\sqrt{\mu_e \epsilon_e} \quad \text{and} \quad \eta_e = \sqrt{\frac{\mu_e}{\epsilon_e}}. \tag{9}$$

If the artificial medium is non magnetic, then $\mu_e = \mu_0$ and $\epsilon_e = k_e^2/\omega^2\mu_0$ avoiding the necessity to compute η_e.

III. Numerical Results

A. PEC Dipoles

For a real anisotropic dielectric, the propagation wavenumber, but not the nine elements of the permittivity tensor, is dependent on the direction of propagation [8, ch. 4], [9, ch. 14]. The first set of data will illustrate that this typically also holds reasonably well for artificial dielectrics. As shown in the insert to Fig. 2, the geometry consists of a 3-D array of perfect electric conducting (PEC) dipoles of radius $a = 0.001\lambda_0$ and length $2h = 0.2\lambda_0$ located in free space. They are arranged in a fixed lattice with $d_1 = 0.25\lambda_0$ and $d_2 = d_3 = 0.05\lambda_0$. The artificial dielectric is uniaxial, and ϵ_{xx}^{er} is the only non–unity diagonal permittivity tensor component. The direction of propagation $\hat{\boldsymbol{u}}$ varies with the angle $\theta = 0$ corresponding to broadside, and 90° corresponding to end fire to the dipoles. As a function of the propagation angle θ, the solid line in the bottom figure shows the values of k_e/k_0 obtained from (3) for the root associated with the $\hat{\boldsymbol{x}}$-directed current. The second root is $k_e = k_0$ and is for the $\hat{\boldsymbol{y}}$ polarization. The top figure shows the relative effective permittivity ϵ_{xx}^{er} computed by both the polarization method and the Maxwell's equations method. Note that ϵ_{xx}^{er} ≈2.4 independent of the angle θ, while k_e/k_0 varies from about 1.54 at broadside to 1 at endfire. In real anisotropic media, the wavenumber for propagation angle θ can be evaluated via the *ellipsoid of wave normals* [8, ch. 4], [9, ch. 14]. The result of this method as applied to the 3-D array of dipoles is that for propagation angle θ

$$k_e(\theta) = k_x k_y \sqrt{\frac{1 + \tan^2\theta}{k_y^2 + k_x^2 \tan^2\theta}} \tag{10}$$

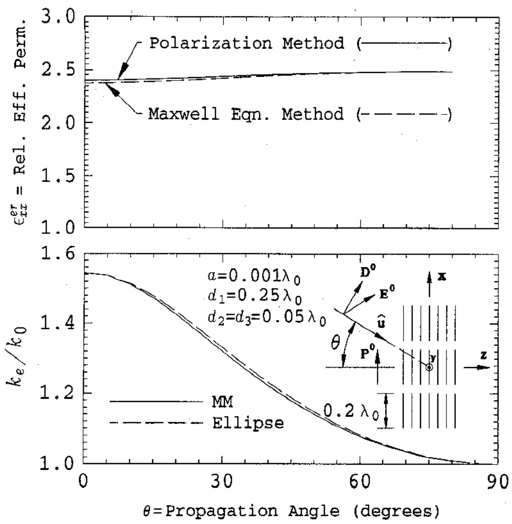

Fig. 2. The normalized effective wavenumber (k_e/k_0) and the relative effective permittivity versus propagation angle θ, for an array of perfectly conducting short dipoles.

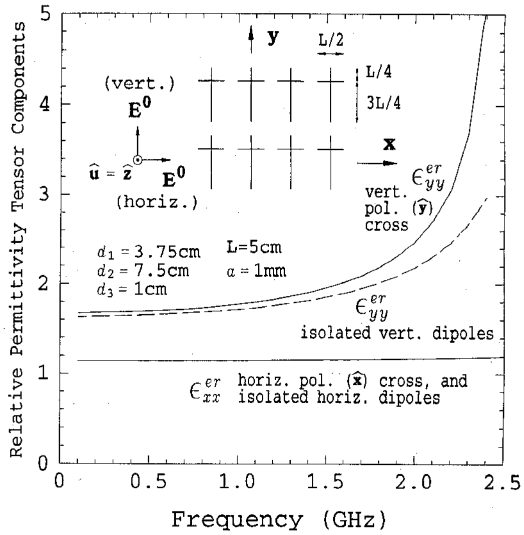

Fig. 3. Dispersion curve for a 3-D array of PEC wire crosses and for isolated vertical and horizontal dipoles.

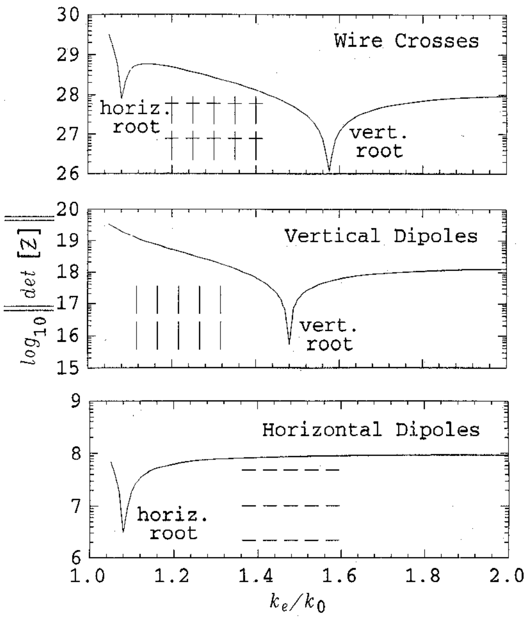

Fig. 4. Magnitude of $|\mathcal{Z}|$ versus normalized effective wavenumber for an array of PEC wire crosses, and for the isolated vertical and horizontal dipole members.

where $k_x \approx 1.54k_0$ (at $\theta = 0$) and $k_y = k_0$ (at $\theta = 90^\circ$). $k_e(\theta)$ computed by (10) is shown by the dashed line in the bottom of Fig. 2, and is seen to be in very close agreement with k_e computed by the PMM from (3).

B. PEC Wire Crosses

The second set of data is for a PEC wire cross, since it is one of the simplest geometries with two distinct roots (different from $k_e = k_0$). As shown in the insert to Fig. 3, the wire crosses of radius $a = 1$ mm have a vertical member of length $L = 5$ cm and a horizontal member of length $L/2 = 2.5$ cm located $L/4 = 1.25$ cm from the top of the vertical member. The wire crosses are arranged in a 3-D lattice with $d_1 = 3.75$ cm, $d_2 = 7.5$ cm, and $d_3 = 1$ cm, and the direction of propagation is along the z-axis. This artificial dielectric is uniaxial with nonunity values for both ϵ_{xx}^{er} and ϵ_{yy}^{er}. The solid lines in Fig. 3 show dispersion curves for ϵ_{xx}^{er} and ϵ_{yy}^{er} for the wire cross, while the dashed lines are for the isolated vertical or horizontal members of the cross. Note that a vertical or $\hat{\boldsymbol{y}}$ polarized wave will directly induce currents on the vertical member of the cross, and then through mutual coupling currents will be induced on the horizontal member of the cross. For this reason Fig. 3 shows different values of ϵ_{yy}^{er} for the cross as compared to the isolated vertical dipole. By contrast, a horizontal or $\hat{\boldsymbol{x}}$ polarized wave will directly induce currents on the horizontal member of the cross. However, since the vertical member is symmetrically located with respect to the horizontal member, the horizontal currents will not induce currents in the vertical member. For this reason, Fig. 3 shows the same values of ϵ_{xx}^{er} for the cross as compared to the isolated horizontal dipole. This effect can also be observed in Fig. 4, which shows the magnitude of the determinant of the impedance matrix $|\mathcal{Z}(k_e)|$ versus the normalized effective wavenumber k_e/k_0 for the array of PEC wire crosses (top figure), as well as for the arrays of isolated vertical (middle figure) and horizontal (bottom figure) dipoles, at the frequency of 2 GHz. The wire cross has two roots at $k_e/k_0 \approx 1.08$ and 1.58, corresponding to horizontal and vertical polarization, respectively. By contrast the isolated vertical and horizontal dipoles show only one root (the other is a free space root $k_e = k_0$).

C. Bent PEC Wires

The next set of data will illustrate a simple bent wire element geometry which results in nonzero off-diagonal elements in the effective permittivity tensor. As shown in the insert to Fig. 5, the geometry consists of a bent PEC wire of total length $3L = 30$ cm and radius $a = 1$ mm. The bent wires are arranged in a 3-D lattice with spacings $d_1 = 12.5$ cm, $d_2 = 22.5$ cm, and $d_3 = 2.5$ cm. An $\hat{\boldsymbol{x}}$ polarized electric field incident upon the bent wire will induce $\hat{\boldsymbol{x}}$ directed currents on the horizontal section and $\hat{\boldsymbol{y}}$ directed currents on the two vertical sections. These currents will radiate both $\hat{\boldsymbol{x}}$ and $\hat{\boldsymbol{y}}$ polarized

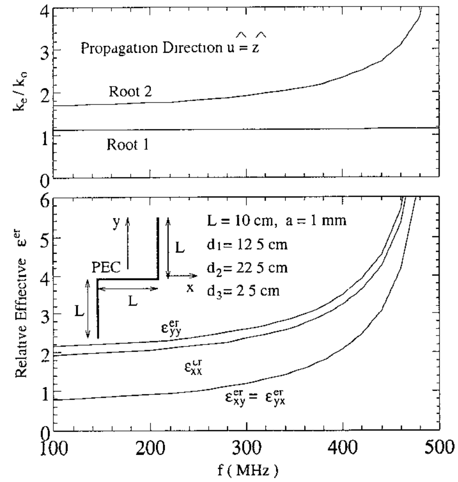

Fig. 5. Dispersion curves for a bent PEC wire geometry.

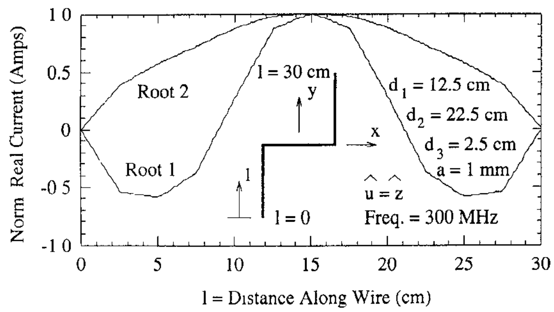

Fig. 6. The two current modes for a bent PEC wire geometry.

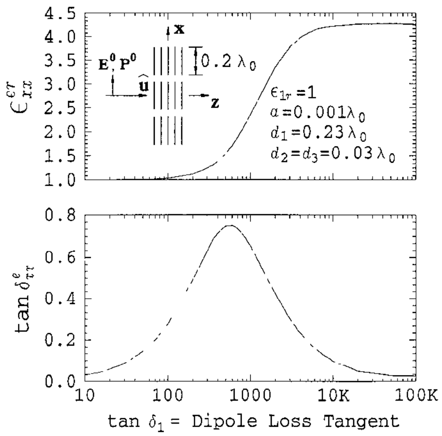

Fig. 7. Relative effective permittivity and loss tangent for a 3-D array of lossy dielectric dipoles.

electric fields, thus producing a nonunity ϵ_{xx}^{er} and a nonzero ϵ_{xy}^{er}. For propagation in the $\hat{\boldsymbol{u}} = \hat{z}$ direction, the top curve in Fig. 5 shows the normalized effective wavenumber k_e/k_0 versus frequency for the two distinct nonfree space roots. The frequency is swept from 100–500 MHz, corresponding to total wire lengths of $0.1\lambda_0 \leq 3L \leq 0.5\lambda_0$. Note that the Root 1 effective wavenumber is nearly constant across the frequency range, whereas the Root 2 effective wavenumber increases rapidly as the total wire length approaches $3L = 0.5\lambda_0$. Fig. 6 shows the two current modes induced on the bent wire at a frequency of 300 MHz. The Root 1 current mode is essentially $+\hat{\boldsymbol{x}}$ and $-\hat{\boldsymbol{y}}$ directed, whereas the Root 2 current mode is $+\hat{\boldsymbol{x}}$ and $+\hat{\boldsymbol{y}}$ directed, similar to the current mode on a straight dipole. The electromagnetic fields of these two modes will be plane waves propagating through the artificial media in the same direction, but with orthogonal polarizations. The bottom curve in Fig. 5 shows the (nonzero and nonunity) relative effective permittivity tensor components versus frequency. The results computed by the Maxwell's Equations method and the polarization method are identical. Also, the numerical results showed that ϵ_{xy}^{er} and ϵ_{yx}^{er} are nearly identical, thus illustrating a similarity between real and artificial media [9, ch. 14.1].

D. Lossy Dielectric Dipoles

The next set of data will illustrate the design of a lossy array of dipoles to maximize the loss of the artificial medium. As shown in the insert to Fig. 7, at $f = 300$ MHz ($\lambda_0 = 1$ m), the geometry consists of lossy dielectric dipoles of length $2h = 0.2\lambda_0$ and radius $a = 0.001\lambda_0$, arranged in a 3-D lattice with spacings $d_1 = 0.23\lambda_0$ and $d_2 = d_3 = 0.03\lambda_0$. Propagation is in the $\hat{\boldsymbol{u}} = \hat{z}$ direction, and polarization is in the $\hat{\boldsymbol{x}}$ direction. The dipoles have relative dielectric constant $\epsilon_{1r} = 1$, and the problem is to choose the dipole loss tangent, $\tan\delta_1$, to maximize the effective loss tangent of the artificial medium. Fig. 7 shows the relative effective permittivity ϵ_{xx}^{er} and effective loss tangent $\tan\delta_{xx}^{e}$ of the artificial medium versus dipole loss tangent for $10 \leq \tan\delta_1 \leq 100{,}000$. Note that as the dipole loss tangent increases, the artificial dielectric effective loss tangent initially also increases, and reaches a maximum of $\tan\delta_{xx}^{e} \approx 0.75$ for a dipole loss tangent of $\tan\delta_1 \approx 600$.

E. Dielectric Weave

The data in this section show the dispersion characteristics of the effective permittivity of a *dielectric weave*, a geometry which has current that flows between adjacent lattice cells. As shown in the insert to Fig. 8, the geometry consists of stacked or layered square grids of dielectric rods. The dielectric rods have relative permittivity $\epsilon_{1r} = 10$ and radius $a = 2$ mm. The grid dimensions are $d_1 = d_2 = L = 5$ cm, and are spaced a distance of $d_3 = 6$ mm apart. Curves are shown for lossless dielectric rods, and also for lossy rods of loss tangent $\tan\delta_1 = 1$. Propagation is along the z-axis, and due to symmetry considerations, the medium is uniaxial with $\epsilon_{xx}^{er} = \epsilon_{yy}^{er}$ and $\epsilon_{zz}^{er} = 1$. Fig. 8 shows the relative effective permittivity $\epsilon_{xx}^{er} = \epsilon_{yy}^{er}$ and effective loss tangent $\tan\delta_{xx}^{e} = \tan\delta_{yy}^{e}$ of the artificial medium for frequency varying up to 3 GHz (corresponding to a grid size of $L = 0.5\lambda_0$) for dielectric rod loss tangent values of $\tan\delta_1 = 0$ and 1. Note that the relative effective permittivity and effective loss tangent are almost constant across the given frequency range, due to essentially constant current in the dielectric rods.

F. Graphite–Epoxy 2-D Composite Medium

This section considers a modern composite material consisting of very thin graphite fibers embedded in an epoxy host binding material. The graphite fibers are modeled as material wires of infinite length in the x direction with radius $a = 3.2\,\mu$m, spaced in a square 2-D lattice with $d_2 = d_3 = 7.5\,\mu$m. The conductivity of the graphite fibers is 71.4 K℧/meter and

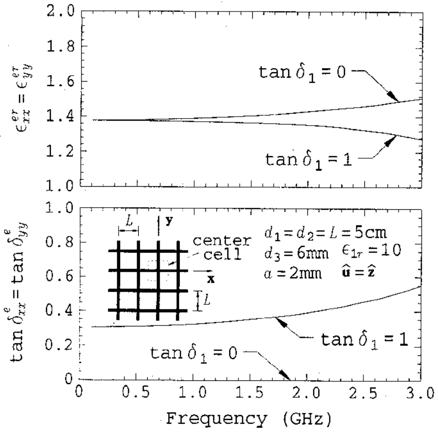

Fig. 8. Dispersion curves for a dielectric weave geometry with lossy and lossless wires.

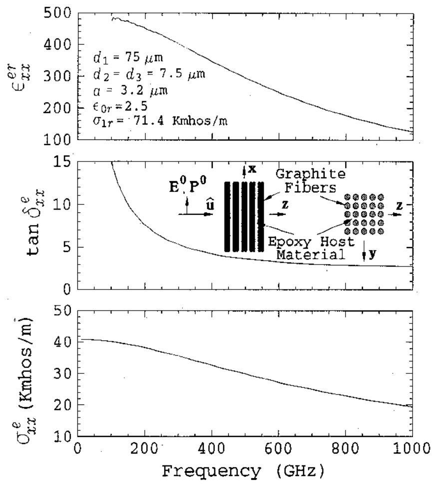

Fig. 9. Dispersion curves for a composite graphite–epoxy material.

the permittivity of the host epoxy material is $\epsilon_{0r} = 2.5$. Fig. 9 shows the computed dispersion characteristics of the composite material. Note that at low frequencies, the effective conductivity is very close to what results from using a simple *fill factor* formula based on a ratio of the area occupied by the graphite fibers to the area occupied by a 2-D lattice cell. That is, for low frequencies, the effective conductivity is approximately given by

$$\sigma_{xx}^e \approx \frac{A_{\text{fiber}}}{A_{\text{cell}}}\sigma_{\text{fiber}} = \frac{\pi a^2}{d_y\, d_z}\sigma_1. \tag{11}$$

Applying (11) to the graphite–epoxy composite medium results in $\sigma_{xx}^e = 40.8\,\text{K℧/meter}$, agreeing very closely with the low frequency results of Fig. 9.

IV. Summary

This paper has considered the PMM analysis of an artificial medium. In general for an anisotropic artificial medium there are plane waves with two distinct roots or wavenumbers, k_e, that can propagation in a given direction. However, in certain special cases one root is a free space root $k_e = k_0$, while in other cases the roots are equal due to problem symmetry. In a real or an artificial anisotropic medium, as the direction of propagation changes, the propagation wavenumber is typically a strong function of angle. By contrast, for a real medium the elements of the tensor constitutive parameters are independent of angle, and for an artificial medium they are (typically) almost independent of angle.

References

[1] R. E. Collin, *Field Theory of Guided Waves,* 2nd ed. New York: IEEE Press, 1991,
[2] C. A. Balanis, *Advanced Engineering Electromagnetics,* ch. 2. New York: Wiley, 1989,
[3] J. L. Blanchard, E. H. Newman, and M. E. Peters "Integral equation analysis of artificial media," *IEEE Trans. Antennas Propagat.,* vol. 42, pp. 727–731, May 1994.
[4] M. E. Peters, "Method of Moments analysis of artificial media composed of dielectric wire objects," Ph.D. dissertation, Dept. of Electrical Engineering, The Ohio State University, Columbus, 1994.
[5] J. L. Blanchard, "Integral equation analysis of artificial dielectrics," Ph.D. dissertation, Dept. of Mathematics, The Ohio State University, Columbus, 1991.
[6] E. H. Newman, "A unified theory of thin material wires," *IEEE Trans. Antennas Propagat.,* vol. 39, pp. 1488–1496, Oct. 1991.
[7] J. A. Kong, *Electromagnetic Wave Theory.* New York: Wiley, pp. 1086–1986.
[8] A. Sommerfeld, *Optics, Lectures on Theoretical Physics,* Vol. IV. New York: Academic, 1954.
[9] M. Born and E. Wolf, *Principles of Optics,* 6th ed. New York: Pergamon, 1980.

Matthew E. Peters (S'90–M'93) was born in Marquette, MI, on June 21, 1964. He received the B.S.E.E. degree from Michigan Technological University, Houghton, in 1986, and the M.S. and Ph.D. degrees in electrical engineering from The Ohio State University in 1990 and 1994, respectively.

From 1987 to 1994, he studied electromagnetics as a Graduate Research Associate at the ElectroScience Laboratory at The Ohio State University. His research interests include theoretical and numerical solutions to electromagnetic scattering and radiation problems. Currently, he works as a Research Engineer at The University of Texas Institute for Geophysics, Austin, where he is involved with geophysics surveying and remote sensing of the polar ice-cap in West Antarctica.

Edward H. Newman (S'67–M'74–SM'86–F'89) was born in Cleveland, OH on July 9, 1946. He received the B.S.E.E., M.S., and Ph.D. degrees in electrical engineering from The Ohio State University in 1969, 1970, and 1974, respectively.

Since 1974 he has been a member of the Ohio State University, Department of Electrical Engineering, ElectroScience Laboratory, where he is currently a Professor. His primary research interest is in the development of method of moments techniques for the analysis of general antenna or scattering problems, and he is the primary author of the "Electromagnetic Surface Patch Code" (ESP). Other research interests include printed circuit antennas, antennas in inhomogeneous media, scattering from material coated edges, artificial dielectrics, and chiral media. He has published over 45 journal articles in these areas, and is a coauthor of the IEEE Press book *Computational Electromagnetics (Frequency Domain Model of Moments).*

Dr. Newman is a Fellow of the IEEE, and is a member of Commission B of URSI and the Electromagnetics Institute. He is a recipient of the 1986 and 1992 College of Engineering Research Award, and is a past chairman of the Columbus sections of the IEEE Antennas and Propagation and Microwave Theory and Techniques Societies.